EFFECT OF COPPER INCORPORATION ON STRUCTURAL, OPTICAL AND ELECTRICAL PROPERTIES OF ZINC TELLURIDE FILMS BY IMMERSION IN Cu SOLUTION

A. ALMOHAMMEDI[a*], A. ASHOUR[a,b], E. R. SHAABAN[c]
[a]*Physics Department, Faculty of Science, Islamic University, P. O. Box 170, Al Madinah, Saudi Arabia.*
[b]*Physics Department, Faculty of Science, Minia University, El Minia, Egypt.*
[c]*Physics Department, Faculty of Science, Al-Azhar University, Assuit, 71542, Egypt*

ZnTe thin films were fabricated on glass substrates by electron beam gun technique. For Cu doping, ZnTe films were immersed in $Cu(NO_3)_2.H_2O$ solution (1g/1000 ml) for different period of times (0, 5, 10, 15 and 20 min.). The crystallographic structure, the crystallite size and the lattice strain were studied by the X-ray diffraction pattern. It is observed that the average crystallite size increases with increasing the immersion time (from 42 to 55 nm when immersion time increased from 0 to 20 min.) but the lattice strain decreases (from $3.3x10^{-3}$ to $2.8x10^{-3}$ when the immersion time increased from 0 to 20 min.). The double beam spectrophotometer was adopted to measure the absorbance in wavelength range extended from 400 to 1100 nm for pure and doping of Cu into ZnTe film. The first derivative of absorbance with respect to wavelength was considered for determination the energy gap, which found to be decreased from 2.26 to 2.21 eV with increasing the immersion time of thin film. The electrical measurements by means of I-V measurement in dark and illumination condition and the sheet resistance were studied by using four probe method. The sheet resistance drastically decreased due to Cu diffusion in the ZnTe films. The dark and photocurrents of the treated ZnTe films were found to be greater than that of as deposited.

(Received August 15, 2018; Accepted January 18, 2019)

Keywords: ZnTe thin film, Cu solution, Structure parameters, Energy gap, Electrical properties, Photocurrent

1. Introduction

Thin films of group II–VI semiconductor and their junctions are of considerable technological and scientific interest. Zinc telluride (ZnTe) is one of the members of this group and has been extensively studied for photovoltaic applications. It has direct energy band gap and has a high optical absorption coefficient, which make possible to as back contact for CdTe in CdTe/CdS heterojunction solar cells [1-6]. One of the useful applications of ZnTe is high efficiency stable electrical back contacts and a small valance band discontinuity for CdTe based solar cells, which have required low resistive p-type ZnTe. To finely tune the structural, optical and electrical properties of ZnTe thin films, it is required to add some proper element as dopant in ZnTe. Cu is transition element and can be doped degenerately into ZnTe, which leads to decrease in its electrical resistance. Cu-doped ZnTe films have been studied by Mahabaduge et al. using co-evaporation technique to produce the flexible CdTe based solar cell devices [7]. The improvement in the efficiency of CdS/CdTe solar cell with an additional layer of Cu-ZnTe has also been reported by Li et al. [8]. Several researchers have employed various techniques such as, e-beam evaporation [9], metal organic chemical vapor deposition [10], pulsed laser deposition [11], vertical Bridgman method, [12], electrodeposition (ED) [13–16], chemical vapor deposition [16], thermal evaporation [17], RF and DC sputtering, hot wall evaporation, diffusion, ion-exchange

*Corresponding author: esam_ramadan2008@yahoo.com

process, etc. [18–25]. In the present work, the effect of Cu doping of ZnTe by immersion in $Cu(NO_3)_2.H_2O$ solution for different period of times regarding structural, optical and electrical properties to explore an efficient material for optoelectronics devices.

2. Experimental

Thin film of ZnTe with thickness 200 nm was deposited onto glass substrates (25 mm x 25 mm) maintained at (150 ^oC) by using the electron beam gun (Edward Auto 306), a precursor was ZnTe powder with purity 99.999 %.

The vacuum system was pumped to a pressure of $2x10^{-6}$ Pa. The thickness of the films was kept to be constant at 200 nm (± 5 nm). The substrate was kept at a distance of about 15 cm from the molybdenum boat, and was rotated during the deposition, to get a deposition rate of 2 nm/sec. The thickness of the film and the rates of evaporation were controlled using a quartz crystal monitor DTM 100, attached to the vacuum system. For Cu doping, ZnTe films were immersed in $Cu(NO_3)_2.H_2O$ solution (1g/1000 ml) for different period of times (0, 5, 10, 15 and 20 min.) and the samples were coded as 1-ZT, 2-ZTC, 3-ZTC, 4-ZTC and 5-ZTC, respectively. After immersion, these samples were cleaned in distilled water and dried by hot compressed air. Then the films annealed at 400 ^oC in order to diffuse Cu inside ZnTe film and yield stoichiometric, transparent and uniform films. The structure and phase purity of the powder and film samples were done at room temperature by X-ray diffractometer (XRD, Philips X-ray diffractometry1710), with Ni-filtered CuK_α radiation (λ = 0.15418 nm). The elemental composition of the $Zn_{1-x}Cu_xSe$ films were analyzed by using energy dispersive X-ray spectrometer unit (EDXS) interfaced with a scanning electron microscope (SEM, JOEL XL) operating an accelerating voltage of 30 kV, used for the morphology studies. The relative error of elements determination does not exceed 2 %, during the analysis. Optical characterization of the films has been performed from spectral transmittance through the double beam spectrophotometer (JASCO, V-670). The transmittance measurements were taken at normal incident, in the wavelength range from 400 to 2500 nm. The electrical resistivity of Cu doping, ZnTe films via immersed in $Cu(NO_3)_2.H_2O$ solution for different period of times were measured at room temperature by measuring currents against applied voltage extended from 1 to 10 V using the four-probe technique. The coplanar circular Molybdenum (Mo) metal contacts were deposited on the front face of the films surfaces by thermal evaporation technique. Before the dark measurement, the sample was maintained in dark for 12 hours in order to empty all trapping states. The photocurrent versus the applied voltage of the as deposited and annealed films was illuminated with a tungsten-halogen lamp with 500 W/m^2 output power.

3. Results and discussion

3.1 Elemental composition analysis

Compositions analysis for ZT, 1-ZTC and 3-ZTC films by energy dispersive X-ray spectroscopy (EDXS) were investigated. Fig. 1 displays the EDXS spectra of three films, respectively. The results presented in Fig. 1 evident that all films are consists Zn, Te and Cu that confirming the incorporated of Cu is into ZnTe matrix.

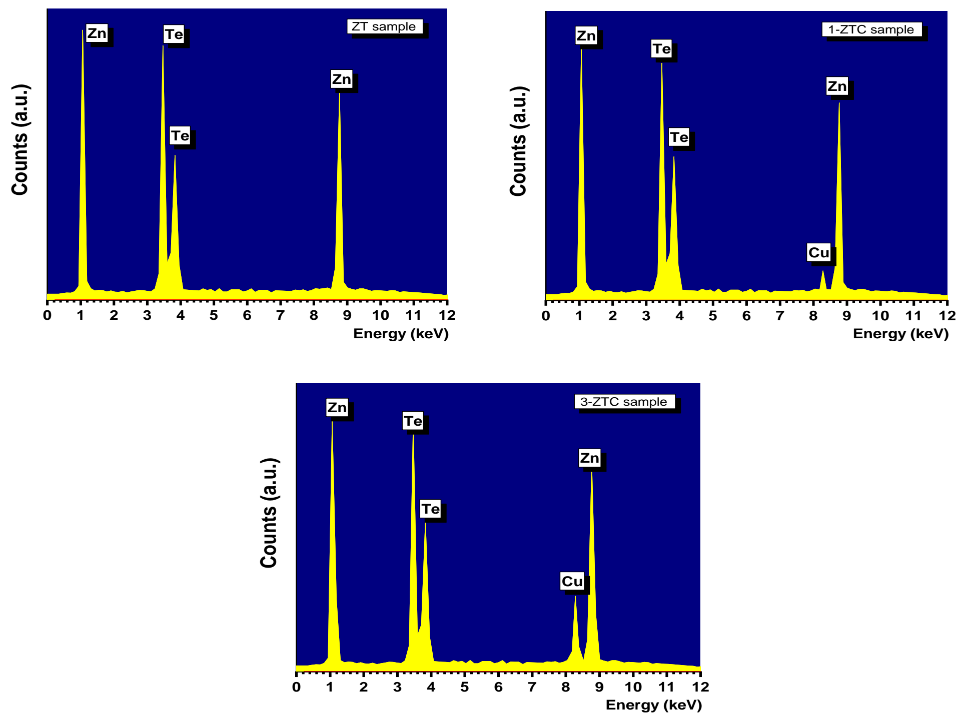

Fig. 1. EDAX patterns of ZnTe:Cu films.

3.2 X-ray diffraction and morphological analysis

Rietveld refinement is a technique for use in the characterization of crystalline materials [26]. The X-ray diffraction of powder samples results in a pattern characterized by reflections (peaks in intensity) at certain positions. The height, width and position of these reflections can be used to determine many aspects of the material's structure. The Rietveld method uses a least squares approach to refine a theoretical line profile until it matches the measured profile. Fig. 2 illustrates Rietveld refinement for ZnTe powder sample.

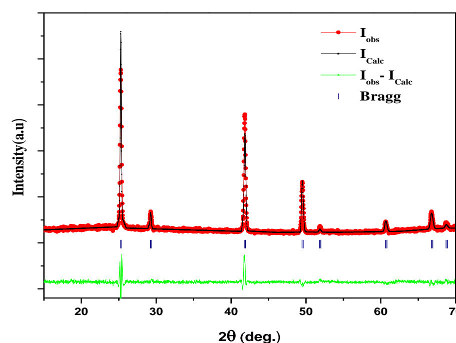

Fig. 2. Rietveld refinement of ZnTe powder sample.

The effect of the different period of immersion times on the structure of ZnTe film was investigated using the X-ray diffractogram as shown in Fig. 3. All diffraction peaks in the XRD pattern for the as-deposited and treated films belongs to zinc blende (JCPDS Data file: 01-0582-cubic) structure of ZnTe with preferred orientation along the (111) plane. Doping of Cu into ZnTe film at different periods of immersion in Cu solution does not significantly affect the crystal structure of ZnTe therefore no secondary phase was appeared for Cu because the atomic radius for both Zn and Cu approximately the same (about 74 pm), which implies that Cu can easily penetrate into ZnTe to substitute Zn position in the crystal lattice resulting that Cu-doping does not change

the crystal structure of ZnTe and single phase has been formed [27–29]. Fig. 3 shows that when the immersion time of ZnTe film increases the diffracted intensity of (111) plane increase, it is evident that Cu doping enhanced the crystallization quality of deposited films. Actually the Cu atoms replace the Zn sites in the host matrix.

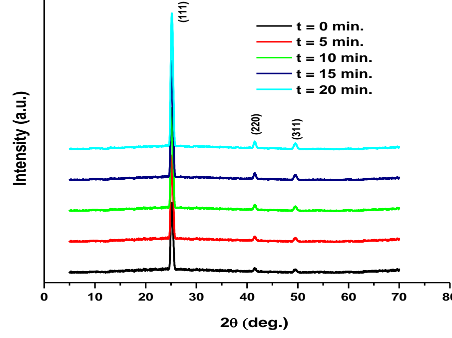

Fig. 3. XRD pattern of as-deposited ZnTe:Cu (0, 5, 10, 15 and 20% min.) thin films.

The peak broadening is due to the instrumentation factor and structure factor that attributed to the crystallite size, the lattice strain.

Both crystallize size (*D*) and lattice strain *(e)* were determined using the Scherrer and Wilson equations [30-32]:

$$D = \frac{0.9\lambda}{\beta \cos\theta} \tag{1}$$

$$e = \frac{\beta}{4\tan\theta} \tag{2}$$

where β is the structural broadening that equals the difference in integral X-ray peak profile width which between the sample and the standard (silicon) and is given as: $\beta = \sqrt{\beta_{obs}^2 - \beta_{std}^2}$.

Fig. 4 shows the comparative look of microstructure parameters (*D* and *e*) of the ZnTe films of different immersion time in Cu solution. It is observed that the average crystallite size increases with increasing the immersion time (from 42 to 55 nm when immersion time increased from 0 to 20 min.) but the lattice strain decreases (from $3.3\text{x}10^{-3}$ to $2.8\text{x}10^{-3}$ when the immersion time increased from 0 to 20 min.). Such a decrease in the lattice strain reflects the decrease in the concentration of lattice imperfections, which might be attributed to the decrease of breadth with increasing immersion time. The crystallize size was found to be the same behavior but lower than that reported by Qeemat Gul et al. [33], which exhibit the crystallite size is 65 and 68 nm for as-deposited and doping by Cu with percentage 10 %, respectively. Such lower values of crystallize size may be attributed to the uniform film preparation by this method, which increases the broadening of the peaks [30-32].

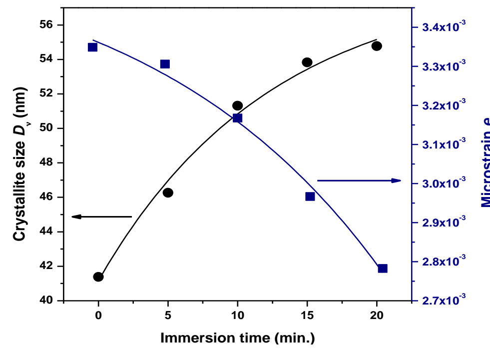

Fig. 4. Crystallite size and lattice strain versus immersion time of ZnTe films.

3.2 Optical absorbance and energy band gap thin films

The double beam spectrophotometer was adopted to measure the absorbance in wavelength range extended from 400 to 1100 nm for pure and doping of Cu into ZnTe film at different periods of immersion in Cu solution (see Fig. 5). When photons are incident on the semiconductor material they will be absorbed only when the minimum energy of photons is enough to excite an electron from the valence band to conduction band or when the photon energy equal to the energy gap of the material. This figure shows that the absorbance shifted towards higher wavelength with increasing the immersion time. In order to extract the energy gap, E_g^{opt} value, the first derivative of absorbance with respect to wavelength was considered. Fig 6 shows the differentiation of absorbance with respect to wavelength as a function of wavelength for all samples. The all peaks that appear in this Figure are due to the electronic transitions from fundamental band edge. The position of the peak has been used to estimate the band gap energy E_g^{opt} [34, 35]. As shown in the inset of Fig. 6, the estimated optical band gap found to be decreased from 2.26 to 2.21 eV with increasing the immersion time of thin film. The same behavior of Cu doping for bandgap in ZnTe thin films was also observed by other researchers [36, 37]. The decreasing in optical band gap may be attributed to the increasing of crystallize size with increasing the immersion time. The crystallize size is made up a large number of atoms, so, the number of overlapping of orbitals or energy level increases and the width of the band gets wider. This will cause a decrease in energy gap between the valance band and the conduction band.

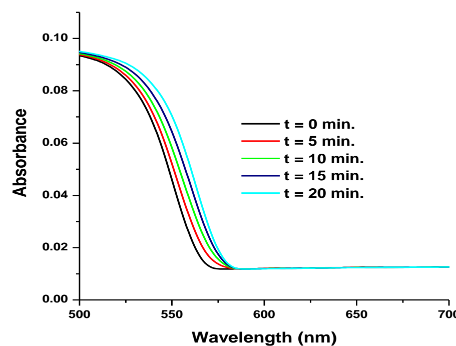

Fig. 5. Five typical absorbance spectra of as-deposited and treated ZnTe thin films.

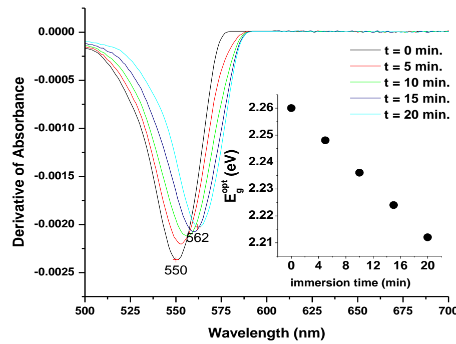

Fig. 6. Absorbance derivative as a function of wavelength, the inset is the energy gap versus immersion time of ZnTe:Cu thin films.

3.3 Electrical properties

The I-V characteristic curve for the pure and doping of Cu into ZnTe film at different periods of immersion in Cu solution has been measured under darkness and illumination as shown in Fig 7 and Fig. 8. Fig. 7 shows that the current increases with increasing the immersion time over all values of applied voltage. Also, the photocurrent versus the applied voltage of each immersion film jump to higher values under the illumination (see Fig. 8). Fig. 9 shows the sheet resistance versus immersion time for the films under dark and illumination. As expected, the sheet resistance decreases with the increasing the time of immersion in Cu solution indicating semiconducting nature of the film. This behavior can be explained as follows: when the immersion time in Cu solution increases, the crystallize size also increases, the grain boundaries decrease and hence the resistance is less. Under photo illumination, the photo generated carriers get trapped at the grain boundaries, this reduces the inter-grain barrier height and carriers can move with less resistance [38, 39].

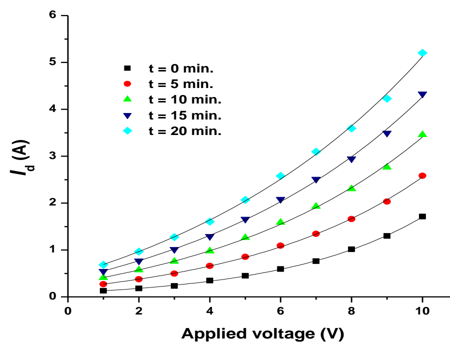

Fig. 7. The dark currents against applied voltage of ZnTe:Cu films.

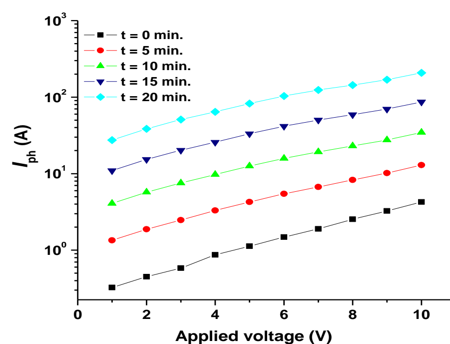

Fig. 8. The photocurrents against applied voltage of the of ZnTe:Cu.films.

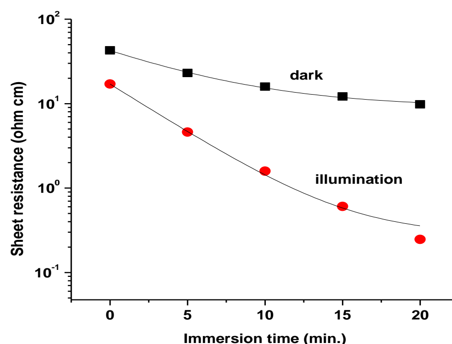

Fig. 9. The sheet resistance against immersion time for both dark and illumination of ZnTe:Cu thin films.

4. Conclusions

ZnTe films with a thickness of 200 nm were fabricated on glass substrates by electron beam gun technique. For Cu doping, ZnTe films were immersed in $Cu(NO_3)_2.H_2O$ solution (1g/1000 ml) for different period of times (0, 5, 10, 15 and 20 min.). Rietveld refinement is used for the characterization of crystalline ZnTe powder sample. All diffraction peaks in the XRD pattern for the as-deposited and treated films belongs to zinc blende with preferred orientation along the (111) plane. The average crystallite size increases with increasing the immersion time (from 42 to 55 nm when immersion time increased from 0 to 20 min.), but the lattice strain decreases (from 3.3 x10^{-3} to 2.8 x10^{-3} when the immersion time increased from 0 to 20 min.).

The first derivative of absorbance with respect to wavelength was considered for determination the energy gap, which found to be decreased from 2.26 to 2.21 eV with increasing the immersion time of thin film. The current increases with increasing the immersion time overall values of applied voltage. Moreover, the photocurrent versus the applied voltage of each annealed film jump to higher values under the illumination.

Acknowledgments

The authors are grateful to Assiut University and Al-Azhar University (Assiut branch) for supporting with the experimental measurements. In addition, the authors thank the Deanship of Scientific Research at Islamic University, Al Madinah, Saudi Arabia for funding this research via project number: (76/1439 H, 2018).

References

[1] S. V. Borse, S. D. Chavhan, Ramphal Sharma, J. Alloys Compd. **436**, 407 (2007).
[2] J. Camacho, A. Cantarero, J. Appl. Phys. **92**, 10 (2002).
[3] P. V. Meyers, Sol. Cell **27**, 91 (1989).
[4] U. M. K. Shahed, Z. Shimin, J. Electrochem. Soc. **142**, 2539 (1995).
[5] H. Zhou, A. Zebib, S. Trivedi, W. M. B. Duval, J. Cryst. Growth **167**, 534 (1996).
[6] T. Ota, K. Takashi, Solid State Electron. **16**, 1089 (1973).
[7] H. P. Mahabaduge, W. L. Rance, J. M. Burst, M. O. Reese, D. M. Meysing, C. A. Wolden, J. Li, J. D. Beach, T. A. Gessert, W. K. Metzger, S. Garner, T. M. Barnes, Appl. Phys. Lett. **106**, 133501 (2015).
[8] J. Li, D. R. Diercks, T. R. Ohno, C. W. Warren, M. C. Lonergan, J. D. Beach, C. A. Wolden, Sol. Energy Mater. Sol. Cells 133, 208 (2015).

[9] M. G. S. B. Ahamed, V. S. Nagarethinam, A. Thayumanavan, K. R. Murali, C. Sanjeeviraja, M. Jayachandran,. J. Mater. Sci. **21**, 1229 (2010)
[10] Z. Li, J. Salfi, C. De Souza, P. Sun, S. V. Nair, H. E. Ruda, Appl. Phys. Lett. **97**, 063510 (2010)
[11] M. L. Xu, K. Gao, J. D. Wu, H. Cai, Y. Yuan, S. Prucnal, R. Hubner, W. Skorupa, M. Helm, S. Q. Zhou, Mater. Res. Express **3**, 036403 (2016)
[12] R. Yang, W. Q. Jie, H. Liu, J. Cryst. Growth **400**, 27 (2014).
[13] M. Bouroushian, T. Kosanovic, D. Karoussos, N. Spyrellis, Electrochim. Acta **54**, 2522 (2009).
[15] O. Skhouni, A. El Manoun, M. Mollar, R. Schrebler, B. Mari,Thin Solid Films **564**, 195 (2014).
[16] M. N. Spallart, C. Konigstein, Thin Solid Films **265**, 33 (1995).
[17] P. Heo, R. Ichino, M. Okido, Electrochim. Acta **51**, 6325 (2006).
[18] L. Feng, D. Mao, J. Tang, R. T. Collins, J. U. Trefny, J. Electron. Mater. **25**, 1442 (1996).
[19] T. A. Gessert, A. R. Mason, P. Sheldon, A. B. Swartzlander, D. Niles, T. J. Coutts, J. Vac. Sci. Technol. A **14**(3), 806 (1996).
[20] T. A. Gessert, T. J. Coutts, Photovoltaic Program Review Proceedings, p. 345, 1993.
[21] I. S. Athwal, R. K. Bedi, J. Appl. Phys. **64**(11), 6345 (1988).
[22] S. I. Koboyashi, N. Saito, Jpn. J. Appl. Phys. **19**, 1199 (1980).
[23] Akram K. S. Aqili, Asghari Maqsood, Appl. Surf. Sci. **167**, 73 (2001).
[24] J. Zhang, L. Feng, W. Cai, J. Zheng, Y. Cai, B. Li, L. Wu, Y. Shao, Thin Solid Films **414**, 113 (2002).
[25] W. Wang, G. Xia, J. Zheng, L. Feng, R. Hao, J. Mater. Sci. Mater. Electron. **18**, 427 (2007).
[20] M. Maniv, A. Zangvil, J. Appl. Phys. **49**, 2787 (1978).
[21] B. D. Cullity, Elements of X-ray Diffractions, Addison-Wesley, Reading, MA, 1978, 102.
[22] G. I. Rusu, M. Diciu, C. Pirghie, E. M. Popa, Appl. Surf. Sci. **253**, 9500 (2007).
[23] C. B. Fitzgerald, Appl. Surf. Sci. **247**, 493 (2005).
[24] E. Popa, G.I. Rusu, Phys. Low-Dim. Struct. **7**, 43 (2003).
[25] D. P. Padiyan, A. Marikini, K. R. Murli, Mater. Chem. Phys. **78**, 51 (2002).
[26] H. M. Rietveld, J. Appl. Cryst. **2**, 65 (1969).
[27] Akram K. S. Aqili, Asghari Maqsood, Appl. Surf. Sci. **167**, 73 (2001).
[28] V. S. John, T. Mahalingam, Solid State Electron. **49**, 3 (2005).
[29] A. L. Patterson, Phys. Rev. **56**, 978 (1939).
[30] E. R. Shaaban, I. Kansal, S. Mohamed, Ferreira, Physica B: Condensed Matter. **404**, 3571 (2009).
[31] E. R. Shaaban, J. Alloys Compd. **563**, 274 (2013).
[32] J. Zhang, L. Feng, W. Cai, J. Zheng, Y. Cai, B. Li, L. Wu, Y. Shao, Thin Solid Films **414**, 113 (2002).
[33] Qeemat Gul, M. Zakria, Taj Muhammad Khan, Arshad Mahmood, Amjid Iqbal, Materials Science in Semiconductor Processing **19**, 17 (2014).
[34] Y. Wang, N. Herron, J. Phys. Chem. **95**, 525 (1991).
[35] E. R. Shaaban, A. Almohammedi, E. S. Yousef, G. A. M. Ali, K. F. Chong, A. Adel, A. Ashour, Optik **164**, 527 (2018).
[36] V. S. John, T. Mahalingam, J. P. Chu, Solid State Electron. **49**, 3 (2005).
[37] G. H. Tariq, N. A. Niaz, M. Anis, UR-Rehman, Chalcogenide Letters **11**, 461 (2014).
[38] P. K. Nair, M. T. S. Nair, J. Campos, L. E. Sansores, Sol. Energy Mater. **15**, 441 (1987).
[39] S. Kolhe, S. K. Kulkarni, M. G. Takwale, V. G. Bhide. Sol. Energy Mater. **13**, 203 (1986).